

Light-induced drift of CH₃F in noble gases

G. J. van der Meer, R. W. M. Hoogeveen, and L. J. F. Hermans

Huygens Laboratory, Leiden University, P.O. Box 9504, 2300 RA Leiden, The Netherlands

P. L. Chapovsky

Institute of Automation and Electrometry, U.S.S.R. Academy of Sciences, 630090 Novosibirsk, Union of Soviet Socialist Republics

(Received 9 November 1988)

Using a new and sensitive technique, experiments on light-induced drift are performed on vibrationally excited CH₃F in the buffer gases He, Ne, Ar, Kr, Xe, and CH₃Cl. For the noble buffer gases, the difference in collision frequency between ground- and excited-state CH₃F with respect to the buffer-gas molecules is found to range from 0.14% for He to 0.56% for Xe. For the polar buffer gas CH₃Cl, this value is found to be 0.98%.

I. INTRODUCTION

In 1979 Gel'mukhanov and Shalagin predicted a new phenomenon,¹ which came to be called light-induced drift (LID). This phenomenon is essentially the demixing of a gas mixture consisting of optically absorbing and nonabsorbing (buffer-gas) particles. It can be achieved by tuning a narrow-band laser within the Doppler-broadened absorption profile, such that particles are excited in a velocity-selective way. This yields opposing fluxes of ground-state and excited-state particles. Without a buffer gas, momentum conservation requires that these fluxes cancel. However, in the presence of a buffer gas, a net drift of the absorbing species can arise, since the ground- and excited-state particles "feel" different "friction forces" caused by a state-dependent gas-kinetic collision frequency (or, equivalently, a difference in collision cross section between ground-state and excited-state particles with respect to the buffer gas).

The relative difference in kinetic collision frequency $\Delta v/v$ is essential to the phenomenon of LID. By measuring this quantity, unique information about the internal-state-dependent molecule-molecule interaction can be obtained.

Experimentally, LID has been demonstrated both in atomic² and molecular systems.³ In atomic vapors such as sodium and rubidium, the LID effect can take spectacular forms such as the optical piston^{4,5} and the optical machine gun.^{6,7} For Rb, isotope separation was also achieved.⁸ In molecular systems, LID has been demonstrated in CH₃F (Ref. 9) and NH₃ (Ref. 10). These studies of the phenomenon involved mostly isotopic mixtures.

In this paper we report results of LID in CH₃F noble-gas mixtures. A new technique will be described for measuring LID, which allows concentration differences down to 1 ppm to be detected. Differences in collision frequency between the ground state and the vibrationally excited state of CH₃F with respect to the buffer gases He, Ne, Ar, Kr, and Xe are presented. In order to compare our results with earlier work for polar buffer gases, experiments were also performed using CH₃Cl as buffer gas.

II. THEORY OF LID OF MOLECULES

Although the physical mechanism behind LID of molecules is the same as that for atomic vapors, its manifestation and method of observation are quite different. The main reason is a large difference in drift velocity between the two cases. According to a simple random-walk argument given by Werij *et al.*⁵ the drift velocity v_{dr} due to LID can be written as

$$v_{dr} = -\eta \frac{\Delta v}{v} v_L, \quad (1)$$

where v_L is the velocity selected by means of the Doppler effect, η is the fraction of absorbing particles which are excited but have not yet suffered a velocity changing collision, and $\Delta v/v$ the relative difference in kinetic collision frequency. For atomic vapors, where the excitation is electronic, η and $\Delta v/v$ can be rather large ($\sim 10^{-1}$), and drift velocities up to 20 m/s have been detected. By contrast, for molecular systems, where the excitation is rovibrational, both η and $\Delta v/v$ are much smaller ($\sim 10^{-3}$), resulting in drift velocities on the order of 10^{-3} m/s. Such small drift velocities, combined with the relatively small absorption coefficient, prevent the formation of an optical piston in molecular systems. Instead, the drift mechanism will generate a demixing of the absorbing species relative to the buffer gas, which is measured as a concentration difference in a closed-tube configuration.

In this section, a theoretical description of molecular LID will be given in which two assumptions are made. First we assume that the collision rate for vibrational-state-changing collisions, ν_{vib} , is much smaller than the rate for velocity changing collisions, ν_{kin} . This is correct for CH₃F, where collisional deexcitation in the bulk takes place at a very low rate,¹¹ while the radiative lifetime is very long, ~ 1 s; consequently, under the conditions of the experiment, deexcitation takes place in molecule-wall collisions. Second, the collision rate for rotational-state-changing collisions, ν_{rot} , is assumed to be much larger than ν_{kin} . This implies that the rotational quantum number does not have to be taken into account, and a two-level description suffices. For our CH₃F-noble-gas sys-

tems, this may in general not be the case. From the homogeneous linewidth, it can be derived that v_{rot} is only somewhat larger than v_{kin} . However, since a Q -branch transition ($\Delta J=0$ upon excitation) is studied in our experiments, the J distribution does not have to be taken into account. Consequently, the model for molecular LID can be expressed in terms of a two-level system (a ground state and a vibrationally excited state).

Under stationary conditions, the equations for the distribution of the molecules over velocity \mathbf{v} in the vibrationally excited state $n_e(\mathbf{v})$ and the ground state $n_g(\mathbf{v})$ are as follows:

$$\mathbf{v} \cdot \nabla n_e(\mathbf{v}) = \sum_{\beta=g,e,b} S_e^\beta(\mathbf{v}) + np(\mathbf{v}), \quad (2)$$

$$\mathbf{v} \cdot \nabla n_g(\mathbf{v}) = \sum_{\beta=g,e,b} S_g^\beta(\mathbf{v}) - np(\mathbf{v}), \quad (3)$$

where $S_\alpha^\beta(\mathbf{v})$ is the collision integral for molecules in state α ($\alpha=g,e$) colliding with either absorbing particles (in state $\beta=g,e$) or buffer-gas particles ($\beta=b$). Furthermore, $n = n_g + n_e$ is the density of absorbing particles and $np(\mathbf{v})d\mathbf{v}$ is the contribution to the net number of absorbed photons per unit time per unit volume due to the particles with velocity between \mathbf{v} and $\mathbf{v}+d\mathbf{v}$. Deexcitation is not incorporated in Eqs. (2) and (3), since it is assumed that the deexciting molecules have a Maxwellian velocity distribution.

For the calculation of the concentration difference over a closed tube, we multiply Eqs. (2) and (3) by \mathbf{v} , integrate over velocity space, and add the ground- and excited-state equation

$$\int d\mathbf{v} \mathbf{v} [\mathbf{v} \cdot \nabla n(\mathbf{v})] = \int d\mathbf{v} \mathbf{v} [S_g^b(\mathbf{v}) + S_e^b(\mathbf{v})], \quad (4)$$

with $n(\mathbf{v}) = n_g(\mathbf{v}) + n_e(\mathbf{v})$. In Eq. (3) we have taken

$$\int d\mathbf{v} \mathbf{v} [S_g^g(\mathbf{v}) + S_g^e(\mathbf{v}) + S_e^g(\mathbf{v}) + S_e^e(\mathbf{v})] = 0, \quad (5)$$

because of momentum conservation. The right-hand side of Eq. (4) equals (apart from the molecular mass) the force between excited and nonexcited particles. This force must be directed along the relative velocity between the particles (when one neglects the small nonsphericity of the interaction). As in Ref. 12 we will use the relation

$$\int d\mathbf{v} \mathbf{v} S_\alpha^\beta(\mathbf{v}) = -v_\alpha^\beta n_\alpha (\mathbf{u}_\alpha - \mathbf{u}_\beta), \quad (6)$$

where \mathbf{u}_α is the average velocity of the particles in level α . The coefficients v_α^β have the meaning of collision rates. Generally these rates depend in a complex way on the velocity distribution. We will neglect this dependence. The validity of this is discussed in Ref. 13.

These assumptions permit a strong simplification of Eq. (4), which now can be written as

$$\int d\mathbf{v} \mathbf{v} [\mathbf{v} \cdot \nabla n(\mathbf{v})] = -v_e^b n_e (\mathbf{u}_e - \mathbf{u}_b) - v_g^b n_g (\mathbf{u}_g - \mathbf{u}_b). \quad (7)$$

In the stationary state in a closed tube, the net fluxes vanish, so that $\mathbf{u}_b = 0$ and $\mathbf{u}_g n_g + \mathbf{u}_e n_e = 0$. Consequently, Eq. (7) can be written as

$$\int d\mathbf{v} \mathbf{v} [\mathbf{v} \cdot \nabla n(\mathbf{v})] = (v_g^b - v_e^b) n_e \mathbf{u}_e. \quad (8)$$

In a molecular system the LID effect is small, such that the total velocity distribution of the absorbing particles can be approximated by a Maxwellian. Using this, Eq. (8) can be written as

$$\frac{1}{2} v_0^2 \nabla n = (v_g^b - v_e^b) n_e \mathbf{u}_e, \quad (9)$$

where $v_0 \equiv \sqrt{2kT/m}$ and n is the total density of absorbing particles.

The flux of absorbing particles in the excited level, $n_e \mathbf{u}_e$, can be found from Eq. (2), since the left-hand side can be neglected with respect to each of the two terms on the right. To this end, Eq. (2) is multiplied by \mathbf{v} and integrated over velocity space, which, using Eq. (6), gives the expression for the flux

$$n_e \mathbf{u}_e = \frac{n \int d\mathbf{v} \mathbf{v} p(\mathbf{v})}{(1 + n_e/n_g) v_e^g + v_e^b}. \quad (10)$$

The denominator may be simplified, since the change in collision frequency upon excitation is small: $(1 + n_e/n_g) v_e^g \approx v_e^a \approx v_a^a$ and $v_e^b \approx v_a^b$, where the label a denotes the absorbing species. Substitution of Eq. (10) in Eq. (9) with $(v_e^b - v_e^g)/v_a^b \equiv \Delta v/v$ yields

$$\frac{1}{2} v_0^2 \nabla n = -\frac{\Delta v}{v} \frac{1}{1 + v_a^a/v_a^b} n \int d\mathbf{v} \mathbf{v} p(\mathbf{v}). \quad (11)$$

For the function $\int d\mathbf{v} \mathbf{v} p(\mathbf{v})$, it is convenient to use the form¹⁴

$$\int d\mathbf{v} \mathbf{v} p(\mathbf{v}) \equiv P v_0 \varphi(\Omega) \frac{\mathbf{k}}{k}, \quad (12)$$

with \mathbf{k}/k the direction of the wave vector and $P = \int d\mathbf{v} p(\mathbf{v})$. The detuning function $\varphi(\Omega)$ can be expressed as¹⁴

$$\varphi(\Omega) = \frac{\text{Re}[z w(z)]}{\text{Re}[w(z)]}, \quad (13)$$

with

$$z = \frac{\Omega}{k v_0} + i \frac{\Gamma_B}{k v_0} \quad (14)$$

and

$$w(z) = e^{-z^2} \left[1 + \frac{2i}{\sqrt{\pi}} \int_0^z dt e^{-t^2} \right], \quad (15)$$

where $\Omega = 2\pi(\nu_L - \nu_0) = k\nu_L$ is the detuning between the laser frequency ν_L and the transition frequency ν_0 , and Γ_B is the homogeneous linewidth. The validity of Eq. (11) for describing LID has been checked in detail in Ref. 9 for the limit $n \ll n_b$, and in Ref. 15 for the limit $n \gg n_b$. The detuning function corrects for the loss of velocity selectivity due to broadening of the absorption profile. In the limit that Γ_B vanishes (δ -peak excitation), the expression for $\varphi(\Omega)$ reduces to $\Omega/kv_0 = \nu_L/\nu_0$. The behavior of $\varphi(\Omega)$ for nonzero Γ_B is shown graphically in Fig. 1(a).

The product $h\nu_L nP$ corresponds to the power absorbed by the gas per unit volume, which equals $(\mathbf{k}/k) \cdot \nabla I$, where I is the intensity. Restricting ourselves to the one-dimensional situation with \mathbf{k} parallel to the x axis, integration of (11) over the length L of the tube gives

$$\Delta n = -\frac{\Delta\nu}{\nu} \frac{1}{1+\nu_a^a/\nu_a^b} \frac{2\Delta I}{h\nu_L\nu_0} \varphi(\Omega), \quad (16)$$

where $\Delta n \equiv \int_0^L \nabla_x n \, dx$ is the drop in absorbing gas density along the length of the tube and ΔI is the absorbed light intensity. In deriving Eq. (16) from (9), it is assumed that $\varphi(\Omega)$ is independent of the position in the tube, which is correct for small absorption (or, in case of large absorption, for small power broadening). In this case, the detuning behavior of Δn is completely determined by the

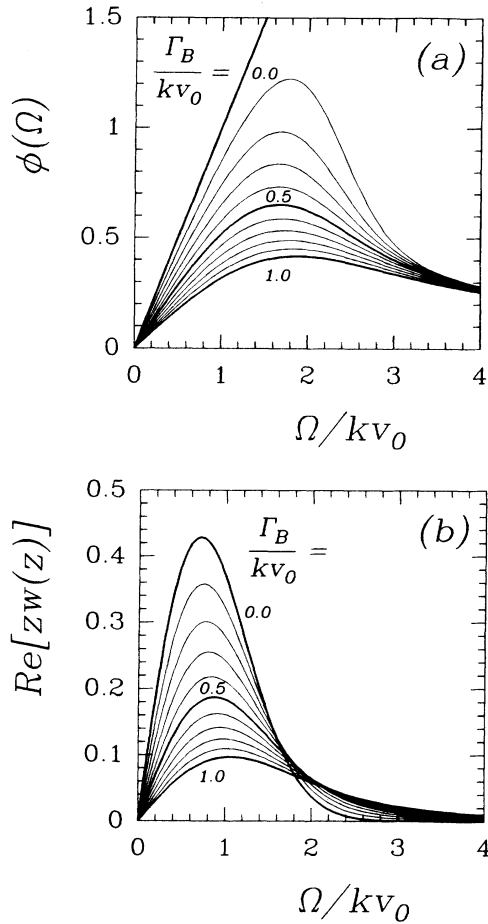


FIG. 1. (a) The detuning function $\varphi(\Omega)$ defined in Eq. (13) for various degrees of homogeneous broadening Γ_B . It determines the detuning behavior of Δn if the absorption ΔI is assumed constant; it approaches $\Omega/kv_0 = v_L/v_0$ if Γ_B approaches zero. (b) The function $\text{Re}[zw(z)] = \varphi(\Omega) \text{Re}[w(z)]$. It determines the detuning behavior of Δn if I_{laser} is assumed constant, i.e., if the absorption ΔI follows the Voigt profile $\text{Re}[w(z)]$; it approaches $(\Omega/kv_0) \exp[-\Omega^2/(kv_0)^2] = (v_L/v_0) \exp[-(v_L/v_0)^2]$ if Γ_B approaches zero.

product $\Delta I \varphi(\Omega)$, as seen in Eq. (16). This is illustrated in Fig. 1(b), where this product is shown as a function of Ω for the case that ΔI follows the Voigt profile, i.e., $\Delta I \propto \text{Re}[w(z)]$ [see Eq. (13)].

The correction term ν_a^a/ν_a^b , which is important outside the limit $n \ll n_b$, can be determined from gas-kinetic data (see Appendix). Note that in the limit $n \ll n_b$, Eq. (16) reduces to (1) upon identification of $\eta = \Delta I / (h\nu_L L n \nu_a^b)$, $D \Delta n / L = n v_{\text{dr}}$, with the diffusion coefficient $D \equiv v_0^2 / (2\nu_a^b)$ and $\varphi(\Omega) = v_L / v_0$.

III. EXPERIMENTAL ARRANGEMENT

The experiments were performed on the symmetric top molecule CH₃F. It has an absorption band around 9.5 μm originating from rovibrational excitation (ν_3 mode or C-F stretch). The carbon-12 isotopic species has three absorption lines nearly resonant with a CO₂ laser line^{16,17} (see Fig. 2). From these the $Q(12,3)$ line (i.e., $v=0 \rightarrow 1$, $J=12 \rightarrow 12$, $K=3 \rightarrow 3$) is a rather isolated absorption line in contrast with the $Q(12,2)$ which was used in earlier work.⁹ However, the $Q(12,3)$ has a detuning of 207 MHz from the $P(20)$ line in the 9.6- μm band of the CO₂ laser for the standard isotopic species. Therefore, an extra cavity acousto-optic modulator is used in double-pass configuration to shift the frequency of the laser by +180 MHz. The waveguide CO₂ laser, which is equipped with a grating for line selection and a piezoelectric element for fine tuning, has a tuning range of 260 MHz, so that the Doppler-broadened $Q(12,3)$ absorption profile can be covered. The Doppler width of the absorption line is ≈ 67 MHz full width at half maximum (FWHM). The CH₃F-noble-gas mixture, having a total pressure of 133 Pa, is contained in a temperature-controlled stainless-steel capillary with a length L of 30 cm and a radius R of 1.0 mm. Two thermopile powermeters are applied to measure the laser power upstream and downstream of the cell. This provides a measurement of the absorbed power ($\pi R^2 \Delta I$) in the gas.

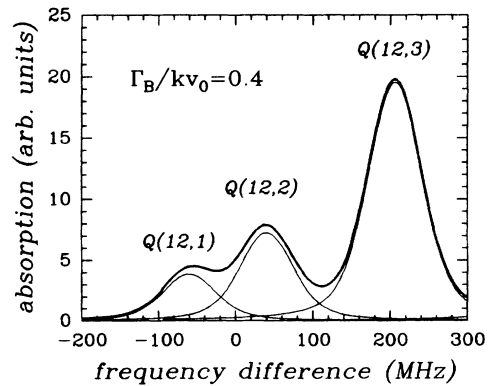


FIG. 2. Absorption spectrum of ¹²CH₃F relative to the $P(20)$ CO₂ laser line in the 9.6- μm band. The homogeneous linewidth Γ_B is chosen to be comparable to the experimental situation. The thin lines represent the individual absorption profiles, the thick line the total absorption profile.

For the detection of the light-induced concentration difference, use is made of the dependence of the thermal conductivity upon composition. This provides a very sensitive differential technique (Refs. 18 and 19). A variation in thermal conductivity is detected by a matched pair of katharometer-type thermistors (ITT, P 15) in the self-heat mode, each of which probes the composition of the gas at one end of the cell (Fig. 3). The resistance of a thermistor can be written as

$$R(T) = R(T_0) e^{B(1/T - 1/T_0)}, \quad (17)$$

where, in our setup, $R(295 \text{ K}) \approx 50 \text{ k}\Omega$ and $B = 3980 \text{ K}$. The thermistor temperature is indicated by T ; the temperature of the surrounding copper block by T_0 . The thermistors are heated up $\Delta T \equiv T - T_0$ with respect to the copper block according to $P_{\text{th}} = \Lambda \Delta T$, with P_{th} a constant electrical power input and Λ the total thermal conduction, which includes heat losses by radiation. A variation in thermal conductivity will give rise to a variation in temperature of the thermistor and thus in its resistance. A differential measurement of the two thermistor resistances is most sensitively achieved by a Wheatstone bridge arrangement. This has the additional advantage that the power P_{th} in each thermistor remains constant in first order, provided that the resistor in series with it is given the same value. In such a scheme, the difference in mole fraction Δx between the two ends of the cell can be related to the resulting difference in resistance ΔR by

$$\Delta x = -\frac{\Lambda}{\Delta T} \left[\frac{\partial \Lambda}{\partial x} \right]^{-1} \left[\frac{\partial R}{\partial T} \right]^{-1} \Delta R, \quad (18)$$

where $\Delta x = \Delta n / (n + n_b)$, with n_b the density of the buffer gas and $n + n_b = p/kT$ constant. The only unknown derivative $\partial \Lambda / \partial x$ can be obtained from a calibration curve, provided by separate measurement in the same setup (Fig. 4). Upon trivial substitutions, one finds

$$\Delta x = \left[\frac{T}{\Delta T} \right]^2 \frac{P_{\text{th}}}{BR} \left[\frac{\partial \Lambda}{\partial x} \right]^{-1} \Delta R. \quad (19)$$

In this experimental setup, variations in mole fraction down to $\Delta x = 1 \text{ ppm}$ can be detected.

IV. RESULTS

In the experiment the frequency of the CO_2 laser, having a typical power of 0.5 W , is slowly scanned through

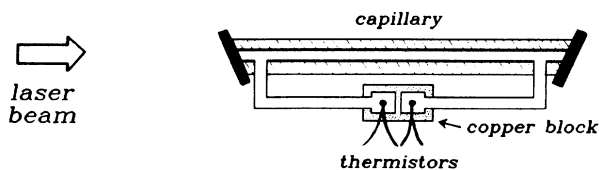


FIG. 3. Schematic illustration of the experimental setup. The capillary is surrounded by a water jacket and has Brewster windows.

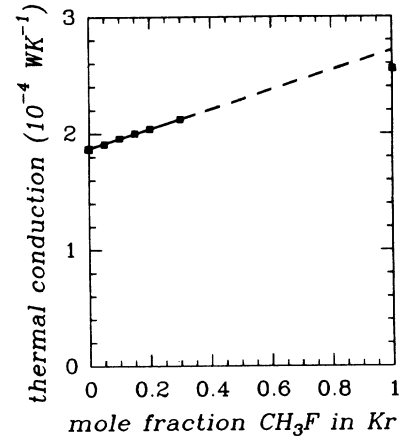


FIG. 4. Measured thermal conduction as a function of mole fraction using Kr as a buffer gas at $p = 133 \text{ Pa}$ and $T = 22.0^\circ\text{C}$. The straight line is the best linear fit through the data at mole fraction $x \leq 0.3$.

the absorption profile of the $Q(12,3)$ line, and the difference in mole fraction Δx is recorded simultaneously (the response time of the system is short, $\sim 15 \text{ s}$). A typical result of a scan, using Kr as a buffer gas, is shown in Fig. 5. The width of the absorption profile is used to derive Γ_B / kv_0 , which determines $\varphi(\Omega)$ [Eq. (13)].

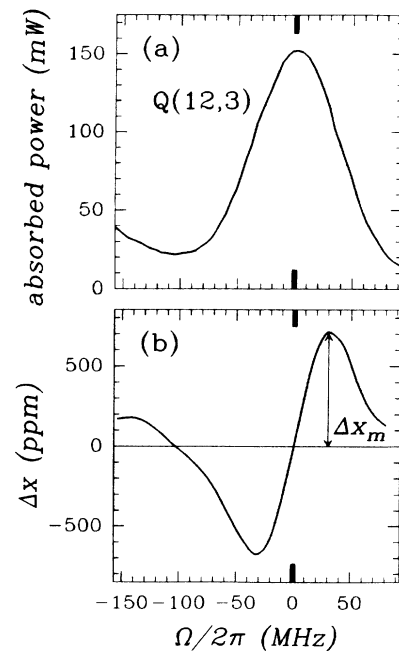


FIG. 5. Typical measurement of the absorption (a) and the LID signal (b) in a mixture of $\text{CH}_3\text{F}/\text{Kr}$ ($x = 0.10$), as a function of detuning. The LID signal is given in terms of difference in mole fraction Δx , with Δx_m the maximum effect at positive detuning. The pressure is 133 Pa , the temperature is 22.0°C , and the laser power $\approx 550 \text{ mW}$.

TABLE I. Measured quantities for the CH₃F–buffer-gas mixtures with mole fraction $x=0.10$. The values of $\Delta\nu/\nu$ given in the last column are averages derived from the $x=0.05$ and 0.10 data.

Buffer gas	I_{laser} (W cm ⁻²)	ΔI at Δx_m (W cm ⁻²)	$\Gamma_B/k\nu_0$	Δx_m (ppm)	$\Delta\nu/\nu$ (10 ⁻³)
He	12.4±0.9	2.91±0.14	0.351±0.043	137±13	+1.4±0.3
Ne	13.4±0.5	2.92±0.12	0.428±0.036	240±11	+2.5±0.3
Ar	13.1±0.8	2.40±0.11	0.389±0.014	453±42	+5.5±0.6
Kr	18.0±0.6	3.40±0.10	0.361±0.026	693±39	+5.6±0.4
Xe	12.7±0.5	2.80±0.12	0.379±0.040	563±16	+5.6±0.5
CH ₃ Cl	11.6±0.6	1.98±0.09	0.581±0.044	656±18	+9.8±0.8

For all CH₃F–noble-gas systems, data were taken for mole fraction $x=0.10$ and $x=0.05$ at a total pressure of $p=133$ Pa. These mole fractions are chosen such that the correction term ν_a^a/ν_a^b in (16) is small ($\leq 15\%$), while the signals are still large enough to be well detected. The two sets of results agree within experimental uncertainty. The data for $x=0.10$ are presented in Table I.

The concentration differences are corrected for spurious effects. The main source of spurious effects arises from pressure differences across the tube, since the thermal conduction depends not only on the composition of the gas mixture, but also on the pressure of the gas at the pressure at which the data were taken (≈ 133 Pa). Such pressure difference arise both from light pressure (even in detuning) and from light-induced viscous flow²⁰ (odd in detuning). The pressure differences occurring in the experiment were measured in parallel with the concentration differences, and straightforward corrections were applied to Δx ranging from 1% for Xe at 15% for He.

The last column of Table I contains the change in collision frequency upon excitation derived from $\Delta x_m = \Delta n_m / (n + n_b)$ using Eq. (16) [with ν_a^a/ν_a^b calculated according to Eq. (A3) in the Appendix]. These values of $\Delta\nu/\nu$ are averages of the values obtained from the 0.05 and 0.10 data.

When comparing our results for the difference in collision frequency with those obtained in earlier work, where the nonabsorbing isotope was used as the buffer gas,⁹ a large difference is noticed [for an isotopic mixture $\Delta\nu/\nu=1.09\pm 0.14\%$ (Ref. 9)]. This difference must be attributed to the dipole moment of the buffer gas, since the dipole moment of CH₃F is known to increase by 2.5% upon vibrational excitation. The validity of this conjecture was verified by performing experiments using CH₃Cl as the buffer gas, which has a dipole moment approximately equal to that of CH₃F [1.90 D (Ref. 21) compared to 1.86 D for CH₃F (Ref. 22)]. Indeed, in this system the change in collision frequency is found to be the same within experimental uncertainties as for the isotopic mixture investigated in Ref. 9 (see Table I).

Our results for the relative difference in collision frequency in CH₃F–noble-gas mixtures can be compared with an estimate given by Lawandy.²³ In that paper, an expression in terms of the rigid sphere radius σ is given:

$$\frac{\Delta\nu}{\nu} = \left[\frac{\sigma_e + \sigma_b}{\sigma_g + \sigma_b} \right]^2 - 1, \quad (20)$$

where the ratio σ_g/σ_b is calculated from virial coefficients and the ratio σ_e/σ_g is estimated from rotational constants. When substituting the values for CH₃F, one finds that the rigid-sphere expression (20) gives the correct order of magnitude for the CH₃F–noble gas systems, but fails to correctly describe the dependence of $\Delta\nu/\nu$ upon the noble-gas radius. This illustrates that a hard-sphere description is inadequate and that the role of the potential well depth has to be taken into account.

ACKNOWLEDGMENTS

The authors would like to thank G. Nienhuis, J. P. Woerdman, E. R. Eliel, N. M. Lawandy, A. M. Shalagin, and A. K. Popov for fruitful discussions and R. J. C. Spreeuw for his part in the experiments. The work is part of the research program of the Foundation for Fundamental Research on Matter (FOM) and was made possible by financial support from the Netherlands Organization for Scientific Research (NWO).

APPENDIX

An expression for the term ν_a^a/ν_a^b in Eq. (16) can be derived if the collision frequency is written as

$$\nu_\alpha^\beta = \frac{5}{4} n_\beta \langle v_{\text{rel}} \rangle_{\alpha\beta} \mathcal{E}_{\alpha\beta}, \quad (A1)$$

where $\langle v_{\text{rel}} \rangle_{\alpha\beta} \equiv \sqrt{8kT/\pi\mu}$ is the mean relative velocity of molecules α with respect to molecules β , μ the reduced mass, and $\mathcal{E}_{\alpha\beta}$ the kinetic cross section of molecules β with regard to molecules α .²⁴ No large error will be introduced if combination rules (frequently used for rigid spheres) are now used in the ratio $\mathcal{E}_{aa}/\mathcal{E}_{ab}$. With $\sqrt{\mathcal{E}_{ab}} = \frac{1}{2}(\sqrt{\mathcal{E}_{aa}} + \sqrt{\mathcal{E}_{bb}})$ one finds

$$\frac{\mathcal{E}_{aa}}{\mathcal{E}_{ab}} = \left[\frac{2}{1 + \sqrt{\mathcal{E}_{bb}/\mathcal{E}_{aa}}} \right]^2. \quad (A2)$$

The correction term v_a^a/v_a^b can now be written as

$$\frac{v_a^a}{v_a^b} = \left(\frac{n}{n_b} \right) \left[\frac{2}{1+m_a/m_b} \right]^{1/2} \left[\frac{2}{1+\sqrt{\mathcal{E}_{bb}/\mathcal{E}_{aa}}} \right]^2, \quad (\text{A3})$$

where the cross-section ratio $\mathcal{E}_{aa}/\mathcal{E}_{bb}$ can be calculated from the viscosities η :²⁴

$$\mathcal{E}_{\alpha\alpha} = \frac{kT}{\langle v_{\text{rel}} \rangle_{\alpha\alpha}} \frac{1}{\eta_{\alpha}}, \quad (\text{A4})$$

with $\alpha = a, b$.

-
- ¹F. Kh. Gel'mukhanov and A. M. Shalagin, *Pis'ma Zh. Eksp. Teor. Fiz.* **29**, 773 (1979) [*JETP Lett.* **29**, 711 (1979)].
- ²V. D. Antsygin, S. N. Atutov, F. Kh. Gel'mukhanov, G. G. Telegin, and A. M. Shalagin, *Pis'ma Zh. Eksp. Teor. Fiz.* **30**, 262 (1979) [*JETP Lett.* **30**, 243 (1979)].
- ³V. N. Panfilov, V. P. Stunin, P. L. Chapovsky, and A. M. Shalagin, *Pis'ma Zh. Eksp. Teor. Fiz.* **33**, 52 (1981) [*JETP Lett.* **33**, 48 (1981)].
- ⁴H. G. C. Werij, J. P. Woerdman, J. J. M. Beenakker, and I. Kuščer, *Phys. Rev. Lett.* **52**, 2237 (1984).
- ⁵H. G. C. Werij, J. E. M. Haverkort, and J. P. Woerdman, *Phys. Rev. A* **33**, 3270 (1986).
- ⁶H. G. C. Werij, J. E. M. Haverkort, P. C. M. Planken, E. R. Eliel, J. P. Woerdman, S. N. Atutov, P. L. Chapovsky, and F. Kh. Gel'mukhanov, *Phys. Rev. Lett.* **58**, 2660 (1987).
- ⁷S. N. Atutov, St. Lesjak, S. P. Pod'jachev, and A. M. Shalagin, *Opt. Commun.* **60**, 41 (1986).
- ⁸A. D. Streater, J. Mooibroek, and J. P. Woerdman, *Appl. Phys. Lett.* **52**, 602 (1988).
- ⁹V. N. Panfilov, V. P. Strunin, and P. L. Chapovsky, *Zh. Eksp. Teor. Fiz.* **85**, 881 (1983) [*Sov. Phys.—JETP* **58**, 510 (1983)].
- ¹⁰A. K. Folin and P. L. Chapovsky, *Pis'ma Zh. Eksp. Teor. Fiz.* **38**, 452 (1983) [*JETP Lett.* **38**, 549 (1983)].
- ¹¹E. Weitz, G. Flynn, and A. M. Ronn, *J. Chem. Phys.* **56**, 6060 (1972).
- ¹²P. L. Chapovsky and A. M. Shalagin, *Kvant. Elektron.* **13**, 2497 (1986) [*Sov. J. Quantum Electron.* **16**, 1649 (1986)].
- ¹³F. Kh. Gel'mukhanov, L. V. Il'ichov, and A. M. Shalagin, *Physica* **137A**, 502 (1986).
- ¹⁴V. R. Mironenko and A. M. Shalagin, *Izv. Akad. Nauk. SSSR, Ser. Fiz.* **45**, 995 (1981) [*Bull. Acad. Sci. USSR, Phys. Ser.* **45**, 87 (1981)].
- ¹⁵A. E. Bakarev, S. M. Ishikaev, and P. L. Chapovsky, *Kvant. Elektron.* **15**, 1318 (1988).
- ¹⁶S. K. Lee, R. H. Schwendeman, R. L. Crownover, D. D. Skatrud, and F. C. DeLucia, *J. Mol. Spectrosc.* **123**, 145 (1987).
- ¹⁷L. C. Bradley, K. L. Soohoo, and C. Freed, *IEEE J. Quantum Electron.* **QE-22**, 234 (1986).
- ¹⁸G. W. 't Hooft, E. Mazur, J. M. Bienfait, L. J. F. Hermans, H. F. P. Knaap, and J. J. M. Beenakker, *Physica* **98A**, 41 (1979).
- ¹⁹E. Mazur, H. J. M. Hijnen, L. J. F. Hermans, and J. J. M. Beenakker, *Physica* **123A**, 412 (1984).
- ²⁰R. W. M. Hoogeveen, G. J. van der Meer, L. J. F. Hermans, A. V. Ghiner, and I. Kuščer, *Phys. Rev. A* (to be published).
- ²¹J. A. Golby and R. J. Butcher, *J. Mol. Spectrosc.* **107**, 292 (1984).
- ²²R. G. Brewer, *Phys. Rev. Lett.* **25**, 1639 (1970).
- ²³N. M. Lawandy, *IEEE J. Quantum Electron.* **QE-19**, 1257 (1983).
- ²⁴P. G. van Ditzhuyzen, B. J. Thijsse, L. K. van der Meij, L. J. F. Hermans, and H. F. P. Knaap, *Physica* **88A**, 53 (1977).